Pergamon

Int. J. Solids Structures Vol. 31, No. 23, pp. 3261–3283, 1994

0020–7683/94 $7.00 + .00

0020–7683(94)00065–4

APPROXIMATE EVALUATION OF THE INTERFACIAL SHEARING STRESS IN CYLINDRICAL DOUBLE LAP SHEAR JOINTS WITH APPLICATION TO DUAL-COATED OPTICAL FIBERS

E. SUHIR
AT & T Bell Laboratories, Murray Hill, NJ 07974, U.S.A.

(*Received* 14 *January* 1993; *in revised form* 24 *February* 1994)

Abstract—A simplified analytical model is developed for the evaluation of the interfacial shearing stress in a cylindrical double lap shear joint, with application to dual-coated optical fiber specimens subjected to pull-out testing, *in situ* measurements of Young's (shear) modulus of the primary coating material, and stripping of the coating from the glass. The objective of the analysis is to assess the effect of the material properties and specimen's geometry on the magnitude and distribution of the shearing stress.

It is shown that the longitudinal distribution of this stress is nonuniform and that, for the given specimen's length, its maximum value increases with a decrease in the thickness of the primary coating. As far as the pull-out testing and Young's modulus evaluations are concerned, it is concluded that, while 1 cm long specimens with approximately 30 μm thick primary coating (such specimens are currently used in pull-out tests) are acceptable, shorter specimens will result in a more uniform stress distribution and, as a consequence of that, in more stable experimental data. As to the coating strippability, it is desirable that the stripping area be short, although satisfactory strippability is often achieved even for long stripping areas. It is concluded that a multiblade stripping tool might be worthwhile to consider if long portions of coating have to be removed from the fiber.

The obtained results can be useful for comparing the adhesive strength of the primary coating in fibers of different lengths and with different coating designs, for the *in situ* evaluation of Young's modulus of the primary coating material from the measured axial displacement of the glass fiber, and for the assessment of the effect of material properties and fiber geometry on the strippability of the fiber coating.

INTRODUCTION

The primary coating adhesion to the glass in dual-coated fibers is being evaluated experimentally on the basis of pull-out tests (Taylor, 1985; Overton and Taylor, 1989). It has been suggested (Overton and Taylor, 1989) that the measured peak tensile force is used to characterize this adhesion. It is clear, however, that although such force might be acceptable as a suitable failure criterion for identical specimens, it is important to be able to determine the maximum stress and the maximum strain energy when comparing the primary coating adhesion to the glass in specimens of different lengths and with different coating designs. At the same time, it has been found [see for instance, Volkersen (1938); Goland and Reissner (1944); Aleck (1949); Grimado (1978); Chen and Nelson (1979); Chang (1983); Du Chen (1983); Suhir (1986), (1989)] that the distribution of the interfacial stress in sufficiently long lap shear joints with stiff interfaces is nonuniform, and that its maxima at the joint's ends are strongly influenced by the material properties and the geometry of the joint. In addition, these maxima, if the adhesive layer is thin, are highly sensitive to the change in the thickness of this layer. A dual-coated optical fiber specimen subjected to tension is, in effect, a cylindrical version of a double lap shear joint, where the primary coating plays the role of the adhesive, and the glass fiber and secondary coating play the role of the adherends. Therefore, if the specimen is too long and/or the primary coating is not thick enough, the elevated sensitivity of the maximum interfacial stress to the inevitable variations in the thickness of the primary coating can result in an elevated variability of the measured pull-out force.

The analysis which follows has been triggered by a wish to find out where 1 cm long dual-coated fiber specimens, which are currently being used in pull-out tests (Overton and Taylor, 1989), are short enough and, with an approximately 30 μm thick primary coating, are compliant enough, to result in a more or less uniform interfacial shearing stress which is not very sensitive to the change in the specimen's length and/or in the primary coating thickness. The objective of the analysis is to develop a simple analytical model for the evaluation of the interfacial shearing stress in cylindrical double lap shear joints, and to apply this model for the assessment of the shearing stress in dual-coated optical fiber specimens. By using the developed model, we intend to determine the effect of the coating materials' properties and the specimen's geometry on the magnitude and the distribution of the shearing stress. Obviously, such a model can be utilized also for the *in situ* evaluation of Young's modulus of the primary coating material from the measured axial displacement of the glass fiber.

In addition to the pull-out testing, we intend to show how the cylindrical double lap shear joint model can be applied for the assessment of the effect of material properties and fiber geometry on the coating strippability.

THEORY

Assumptions

The analysis is based on the following major assumptions.

1. All the materials behave as linearly elastic. This assumption is undoubtedly applicable in the case of *in situ* Young's modulus measurements, when the induced deformations are small. Some recent experimental data (Simoff, 1992) show, however, that the axial displacement of the glass fiber is practically proportional to the applied force up to the very moment of rupture, and therefore the linear approach is thought to be justified for the case of pull-out testing as well.
2. The specimens are ideally circular and the loading is purely collinear to the specimen's axis, i.e. no bending deformations occur.
3. The thermally induced ("residual") stresses and the radial and tangential (circumferential) mechanical stresses, caused by the tensile force, are not accounted for. In other words, it is assumed that the shearing stress can be evaluated without considering other stress categories (Suhir, 1991; Mishkevich and Suhir, 1993).
4. The primary coating material experiences shear only. This assumption is justified by the fact that Young's modulus of the "adhesive" (primary coating) is significantly smaller than Young's moduli of the "adherends" (the glass and the secondary coating) (Suhir, 1988a). In the case in question, such an assumption simply means that the shearing stress $\tau_0(x)$ at the interface between the glass and the primary coating and the shearing stress $\tau_1(x)$ at the interface between the primary and the secondary coatings are inversely proportional to the corresponding radii (Fig. 1):

$$\frac{\tau_0(x)}{\tau_1(x)} = \frac{r_1}{r_0}. \tag{1}$$

Indeed, since no external forces act on the primary coating, this coating has to be in equilibrium under the action of the interfacial shearing stresses only, and therefore the following condition should be fulfilled:

$$2\pi r_0 \int_0^x \tau_0(\xi)\,d\xi - 2\pi r_1 \int_0^x \tau_1(\xi)\,d\xi = 0.$$

The differentiation of this equation with respect to x results in the condition (1).

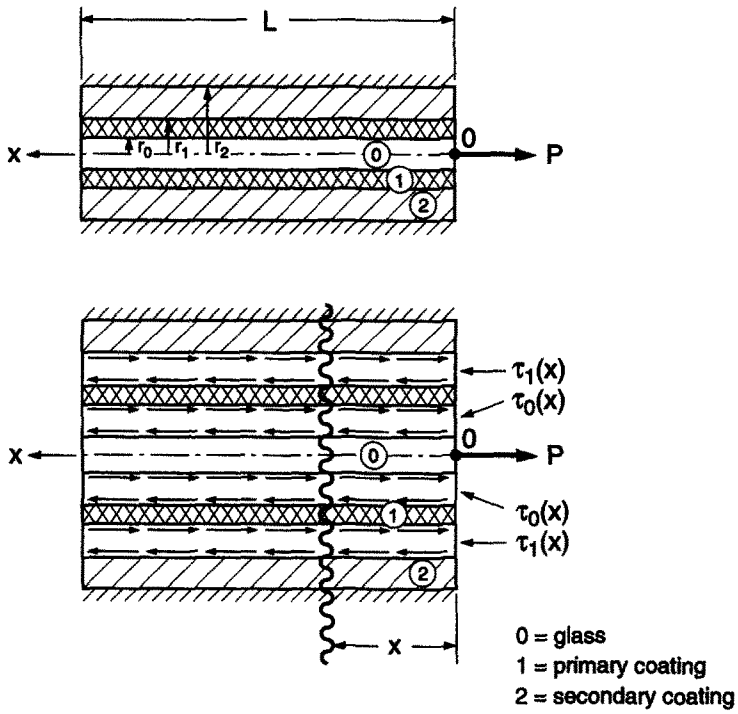

Fig. 1. Optical fiber specimen subjected to tension.

Loading conditions

The following two loading conditions are considered when evaluating the shearing stress in a dual-coated fiber specimen subjected to tension.

Case 1. The specimen is loaded at its end planes, so that the external force is applied to the glass at one end of the specimen, and is equilibrated by a reaction force applied to the secondary coating at the other end (Fig. 2).

Case 2. The specimen is embedded into an epoxy adhesive, so that the external force is applied to the glass fiber at the end of the specimen, i.e. in the same manner as in the previous case, but is equilibrated by a shearing force distributed over the outer lateral surface of the secondary coating (Fig. 3).

The first condition applies to the general case of a cylindrical double lap shear joint, while the second condition is thought to be close to the actual situation taking place during pull-out testing of optical fiber specimens and during *in situ* measurements of Young's modulus of the primary coating.

Case 1. *Specimen loaded at its end planes*

Basic equation. The shearing stress $\tau_0(x)$ on the glass surface of a dual-coated optical fiber specimen loaded at its end planes (Fig. 2) can be determined on the basis of the following condition of compatibility for the longitudinal (axial) interfacial displacements:

$$w_0(x) = w_2(x) - \kappa\tau_0(x). \tag{2}$$

Here $w_0(x)$ are the longitudinal displacements of the points located at the glass surface, $w_2(x)$ are the displacements of the points located at the inner boundary of the secondary coating,

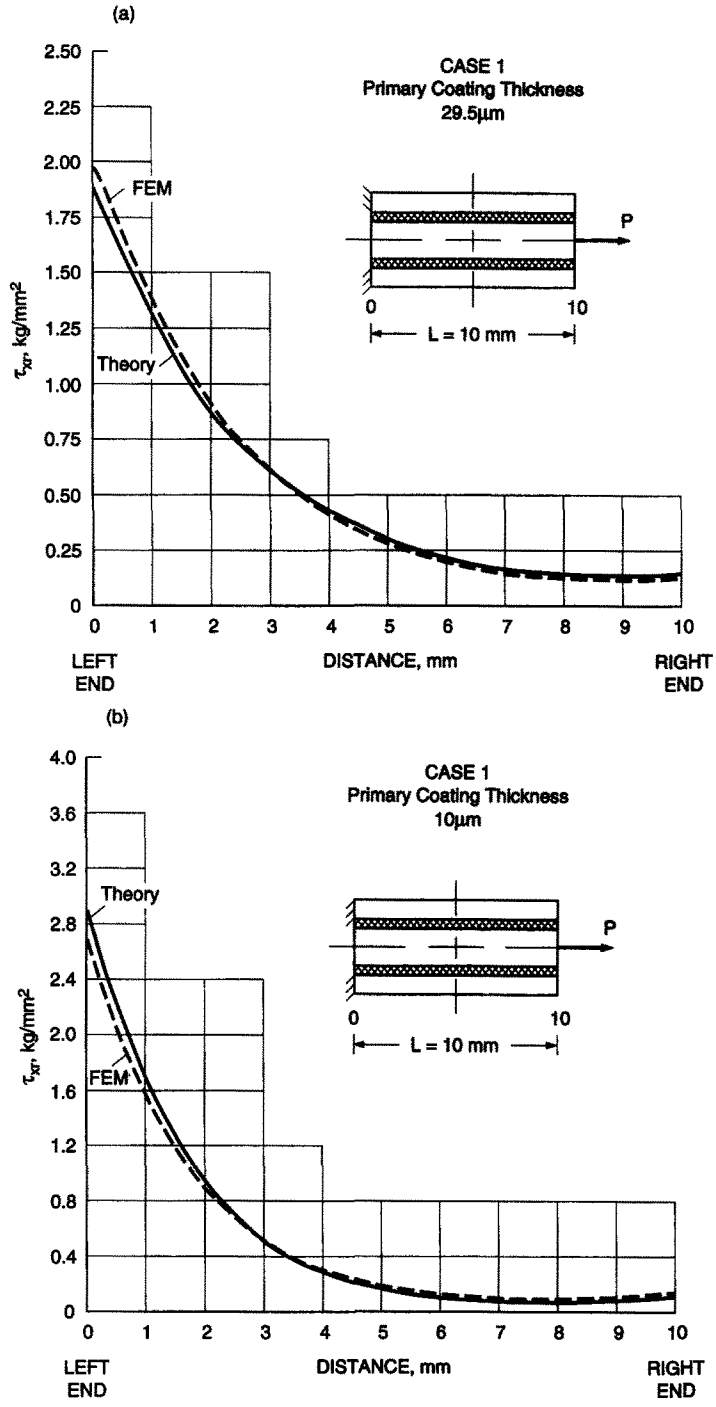

Fig. 2. Optical fiber specimen loaded at its end planes. The primary coating is (a) 29.5 μm thick, (b) 10 μm thick. FEM = finite element method (modeling).

$$\kappa = \frac{r_0}{G_1} \ln \gamma_0 \tag{3}$$

is the longitudinal interfacial compliance of the primary coating (Suhir and Sullivan, 1990), $\gamma_0 = r_1/r_0$ is the radii ratio, $G_1 = E_1/2(1+\nu_1)$ is the shear modulus of the primary coating material, and E_1 and ν_1 are its Young's modulus and Poisson's ratio, respectively.

If the stresses $\tau_0(x)$ and $\tau_1(x)$ were known, then the displacements $w_0(x)$ and $w_2(x)$ could be approximately evaluated using Hooke's law as follows:

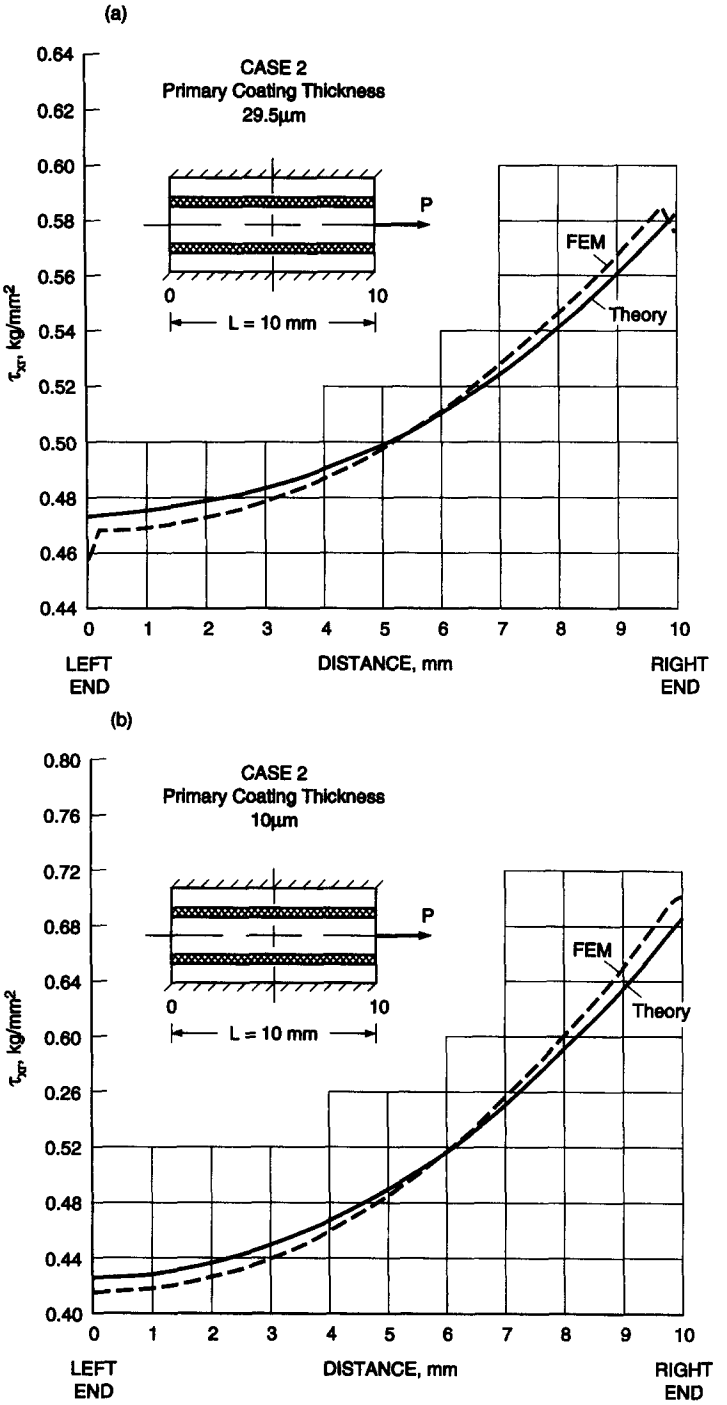

Fig. 3. Optical fiber specimen embedded into an epoxy adhesive. The primary coating is (a) 29.5 μm thick, (b) 10 μm thick. FEM = finite element method (modeling).

$$w_0(x) = \lambda_0 \int_0^x T_0(\xi)\,\mathrm{d}\xi, \quad w_2(x) = \lambda_2 \int_0^x T_2(\xi)\,\mathrm{d}\xi, \tag{4}$$

where

$$T_0(x) = P - 2\pi r_0 \int_0^x \tau_0(\xi)\,\mathrm{d}\xi \tag{5}$$

is the axial force in the glass fiber, P is the external tensile force,

$$T_2(x) = P - T_0(x) \tag{6}$$

is the axial force in the secondary coating,

$$\lambda_0 = \frac{1}{\pi r_0^2 E_0}, \quad \lambda_2 = \frac{1}{\pi(r_2^2 - r_1^2)E_2} \tag{7}$$

are the axial compliances of the glass fiber and the secondary coating, respectively, and E_0 and E_2 are Young's moduli of these materials.

Introducing eqn (4) into the compatibility condition (2) and considering the relationships (1) and (6), we obtain the following equation for the interfacial shearing stress $\tau_0(x)$:

$$\kappa\tau_0(x) + \lambda \int_0^x T_0(\xi)\,\mathrm{d}\xi = \lambda_2 P x, \tag{8}$$

where the force $T_0(x)$ is related to the shearing stress $\tau_0(x)$ by eqn (5), and

$$\lambda = \lambda_0 + \lambda_2 \tag{9}$$

is the total axial compliance of the specimen.

Differentiating eqn (8) with respect to x, we obtain

$$\kappa\tau_0'(x) + \lambda T_0(x) = \lambda_2 P. \tag{10}$$

The next differentiation yields

$$\tau_0''(x) - k^2\tau_0(x) = 0, \tag{11}$$

where the eigenvalue of the problem

$$k = \sqrt{2\pi r_0 \frac{\lambda}{\kappa}} \tag{12}$$

depends on the ratio of the axial compliance λ to the total interfacial compliance κ.

Solution to the basic equation. Equation (11) has the following solution:

$$\tau_0(x) = C_1 \cosh kx + C_2 \sinh kx, \tag{13}$$

where the constants C_1 and C_2 of integration can be determined from the boundary conditions for the force T_0:

$$T_0(0) = P, \quad T_0(L) = 0. \tag{14}$$

As is evident from eqn (10), the conditions (14) are equivalent to the following conditions for the function $\tau_0(x)$:

$$\kappa\tau_0'(0) = -\lambda_0 P, \quad \kappa\tau_0'(L) = \lambda_2 P. \tag{15}$$

Substituting eqn (13) into the conditions (15), we obtain

$$C_1 = \frac{P}{k\kappa}\frac{\lambda_0 \cosh u + \lambda_2}{\sinh u}, \quad C_2 = -\frac{P}{k\kappa}\lambda_0, \tag{16}$$

where the parameter u is expressed as

$$u = kL = L\sqrt{2\pi r_0 \frac{\lambda}{\kappa}}. \tag{17}$$

With the formulae (16), solution (13) can be written as follows:

$$\tau_0(x) = \frac{P}{k\kappa}\frac{\lambda_0 \cosh k(L-x) + \lambda_2 \cosh kx}{\sinh u}. \tag{18}$$

At the specimen ends ($x = 0$ and $x = L$), the shearing stress is

$$\tau_0(0) = \frac{P}{k\kappa}\frac{\lambda_0 \cosh u + \lambda_2}{\sinh u}$$

$$\tau_0(L) = \frac{P}{k\kappa}\frac{\lambda_0 + \lambda_2 \cosh u}{\sinh u}. \tag{19}$$

In the middle of the specimen ($x = L/2$),

$$\tau_0\left(\frac{L}{2}\right) = \frac{P}{2k\kappa}\frac{\lambda}{\sinh u/2}. \tag{20}$$

Special cases. In sufficiently long (large L values) specimens with stiff interfaces (large k values), the parameter $u = kL$ is also large. When it is larger than, say 2.5, the shearing stress in the midportion of the specimen, expressed by formula (20), is very small and the stresses at the specimen's ends, given by formulae (19), become independent of its length:

$$\tau_0(0) = \frac{P}{k\kappa}\lambda_0, \quad \tau_0(L) = \frac{P}{k\kappa}\lambda_2. \tag{21}$$

Since the axial compliance λ_2 of the secondary coating is, as a rule, significantly larger than the axial compliance λ_0 of the glass fiber, the maximum shearing stress takes place at the end $x = L$. Physically, this result can be explained by the fact that the secondary coating, because of its relatively high compliance, transmits the external force to the glass surface within a significantly smaller length than the glass fiber does, thereby resulting in a larger interfacial stress.

In the case of large $u = kL$ values, solution (18) can be simplified as follows:

$$\tau_0(x) = \frac{P}{k\kappa}[\lambda_0 e^{-kx} + \lambda_2 e^{-k(L-x)}]. \tag{22}$$

This formula indicates that in a long specimen with a stiff interface, the shearing stress is very small in the inner portion of the specimen (where x is appreciably greater than zero, but smaller than L), and concentrates at the specimen's ends (where x is close either to zero or to L).

If the compliances λ_0 and λ_2 of the "adherends" were equal, then expression (18) would result in the following formula for the interfacial stress:

$$\tau_0(x) = \frac{P\lambda}{2k\kappa} \frac{\cosh k\left(\frac{L}{2} - x\right)}{\sinh \frac{u}{2}}. \tag{23}$$

In this case, the stress $\tau_0(x)$ is distributed symmetrically with respect to the specimen's mid cross-section $x = L/2$, and the stresses at the specimen's ends are the same:

$$\tau_0(0) = \tau_0(L) = \frac{P\lambda}{2k\kappa} \operatorname{cotanh} \frac{u}{2}. \tag{24}$$

For long specimens with stiff interfaces, these stresses are

$$\tau_0(0) = \tau_0(L) = \frac{P\lambda}{2k\kappa}, \tag{25}$$

i.e. are half the value of the maximum shearing stress in a situation when the compliances λ_0 and λ_2 differ considerably.

It should be pointed out that stiffer "adherends" (glass fiber and the secondary coating) and a more compliant "adhesive" (primary coating) result in lower interfacial stresses. Indeed, using the notation (12) and assuming $\lambda_2 \cong \lambda$, we obtain the second formula in eqn (19) in the form

$$\tau_0(L) = \frac{kP}{2\pi r_0} = \frac{P}{\sqrt{2\pi r_0}} \sqrt{\frac{\lambda}{\kappa}}. \tag{26}$$

This formula indicates that the maximum interfacial stress decreases with a decrease in the total axial compliance λ and an increase in the total interfacial compliance κ. Since in the case of a dual-coated fiber, the axial compliance λ is due primarily to the secondary coating, and the interfacial compliance κ is due mainly to the primary coating, the increase in the stiffness of the secondary coating and in the compliance of the primary coating result in lower interfacial stresses.

Tensile forces in the glass fiber and the secondary coating. Introducing eqn (18) into eqn (5), we obtain the following formula for the tensile force in the glass fiber:

$$T_0(x) = P \frac{\lambda_0 \sinh k(L-x) + \lambda_2(\sinh u - \sinh kx)}{\lambda \sinh u}. \tag{27}$$

Then the tensile force in the secondary coating is

$$T_2(x) = P - T_0(x) = P \frac{\lambda_0[\sinh u - \sinh k(L-x)] + \lambda_2 \sinh kx}{\lambda \sinh u}. \tag{28}$$

Clearly, $T_0(0) = T_2(L) = P$ and $T_0(L) = T_2(0) = 0$.

For long specimens with stiff interfaces ($u > 2.5$), formulae (27) and (28) can be simplified as follows:

$$T_0(x) = \frac{P}{\lambda}[\lambda_0 e^{-kx} + \lambda_2(1 - e^{-k(L-x)})]$$

$$T_2(x) = \frac{P}{\lambda}[\lambda_0(1 - e^{-kx}) + \lambda_2 e^{-k(L-x)}]. \tag{29}$$

In the inner portions of the specimens, where the coordinate x is appreciably larger than zero but smaller than L, these formulae yield

$$T_0 \cong P\frac{\lambda_2}{\lambda}, \quad T_2 \cong P\frac{\lambda_0}{\lambda}, \tag{30}$$

as it is supposed to be in accordance with the Saint-Venant principle; for cross-sections sufficiently remote from the specimen's ends (where the external loading is applied), the distribution of the total force P between the glass fiber and the secondary coating is independent of the actual boundary conditions (i.e. of the actual way in which the force P is applied), and the stiffer element (glass) experiences a proportionally larger force.

Stress concentration factor. When the u value is small (say, smaller than 0.25), formulae (18), (27) and (28) yield

$$\tau_0 = \frac{P}{2\pi r_0 L}, \quad T_0(x) = P\left(1-\frac{x}{L}\right), \quad T_2 = P\frac{x}{L}, \tag{31}$$

i.e. the shearing stress at the interface is distributed uniformly, while the axial forces in the adherends are distributed linearly along the specimen.

Comparing the second formula in (19) for the maximum stress in the general case of a finite interfacial compliance and finite specimen's length with the first formula in (31), we obtain the following expression for the stress concentration factor:

$$k_L = \frac{\tau_0(L)}{\tau_0} = u\frac{\lambda_0+\lambda_2\cosh u}{\lambda \sinh u}. \tag{32}$$

When the u value is large, we have

$$k_L = u\frac{\lambda_2}{\lambda} \cong u = kL.$$

This formula explains the physical meaning of the eigenvalue k, introduced by formula (12). This is, in effect, the ratio of the stress concentration factor k_L in long specimens with stiff interfaces to the specimen's length L.

Strain energy. The strain energy of the deformed primary coating can be assessed by the formula

$$\begin{aligned} V &= \frac{\pi}{G_1}\int_0^L\int_{r_0}^{r_1}\tau^2(r,x)r\,\mathrm{d}r\,\mathrm{d}x \\ &= \frac{\pi}{G_1 r_1^2}\int_0^L \tau_0^2(x)\,\mathrm{d}x\int_{r_0}^{r_1}(r_0+r_1-r)^2 r\,\mathrm{d}r \\ &= \frac{\pi r_0^2}{2G_1}c\int_0^L \tau_0^2(x)\,\mathrm{d}x, \end{aligned} \tag{33}$$

where the factor c is related to radii ratio $\gamma_0 = r_0/r_1$ as

$$c = \frac{1}{6}\frac{(1-\gamma_0^2)(1+\gamma_0^2+4\gamma_0)}{\gamma_0^2}.$$

Substituting eqn (18) into eqn (33) and carrying out the integration, we obtain

$$V \equiv \frac{\pi r_0^2}{G_1 k} c\left(\frac{P}{2k\kappa}\right)^2 \frac{(\lambda_0^2+\lambda_2^2)(\sinh 2u+2u)+4\lambda_0\lambda_2 \sinh u}{\sinh^2 u}, \tag{34}$$

or, since λ_2 is significantly greater than λ_0,

$$V \cong \frac{\pi r_0^2}{G_1 k} c\left(\frac{P\lambda_2}{2k\kappa}\right)^2 \frac{\sinh 2u+2u}{\sinh^2 u}. \tag{35}$$

When the u value is large, the expression (35) for the strain energy can be further simplified as follows:

$$V \cong \frac{\pi r_0^2}{G_1 k} c\left(\frac{P\lambda_2}{2k\kappa}\right)^2. \tag{36}$$

Using the second formula in eqn (21) for the maximum stress, we obtain eqn (36) in the form

$$V \cong \frac{\pi r_0^2}{4G_1 k} c\tau_0^2(L). \tag{37}$$

This formula indicates that the strain energy stored in the primary coating is proportional to the maximum shearing stress squared, and therefore either the strain energy or the maximum shearing stress can be used as an appropriate criterion of the adhesive strength.

Case 2. Specimen embedded into an epoxy adhesive

Basic equation. Examine now a situation when the specimen is embedded into an epoxy adhesive (Fig. 3). In the analysis which follows, we assume that the stresses caused by the thermal contraction mismatch of the epoxy and the specimen need not be accounted for. The effect of such stresses can be minimized, for instance, by introducing longitudinal gaps (cuts) into the epoxy.

The external force P applied to the glass is equilibrated by the shearing load $\tau_2(x)$ distributed over the outer surface of the secondary coating. Then the tensile force in the glass fiber is

$$T(x) = P - 2\pi r_2 \int_0^x \tau_2(\xi)\,d\xi. \tag{38}$$

In the case in question, both the primary and the secondary coatings experience shear loading only, so that $r_0\tau_0(x) = r_2\tau_2(x)$. Therefore, the relationship (38) can be replaced by the formula

$$T(x) = P - 2\pi r_0 \int_0^x \tau_0(\xi)\,d\xi. \tag{39}$$

The longitudinal displacements $w_0(x)$ of the glass fiber can be evaluated in accordance with the first formula in (4), while the longitudinal displacements $w_2(x)$ of the secondary coating

embedded into the epoxy should be put equal to zero. Then the compatibility condition (2) can be written as

$$\lambda_0 \int_0^x T(\xi)\,\mathrm{d}\xi + \kappa\tau_0(x) = 0. \tag{40}$$

Differentiating eqn (40) twice with respect to the coordinate x, we obtain

$$\lambda_0 T(x) + \kappa\tau_0'(x) = 0 \tag{41}$$

$$\tau_0''(x) - k^2\tau_0(x) = 0, \tag{42}$$

where relationship (39) is considered and the notation

$$k = \sqrt{2\pi r_0 \frac{\lambda_0}{\kappa}} \tag{43}$$

is used. Equation (42) coincides with eqn (11) and therefore its solution is expressed by formula (13). The eigenvalue k, however, is different; it is given by formula (43) where the total axial compliance is due to the glass only, but not by formula (12), where this compliance is due to both the secondary coating and the glass.

The force $T_0(x)$ has the following values at the specimen ends:

$$T(0) = P, \quad T(L) = 0. \tag{44}$$

Then eqn (41) results in the following boundary conditions for the shearing stress function $\tau_0(x)$:

$$\kappa\tau_0'(0) = -\lambda_0 P, \quad \tau_0'(L) = 0. \tag{45}$$

Note, the first of these conditions is the same as the first condition in (15), while the second condition is different.

Introducing eqn (13) into eqn (45), we obtain

$$C_1 = \frac{P\lambda_0}{k\kappa}\operatorname{cotanh} u, \quad C_2 = -\frac{P\lambda_0}{k\kappa}, \tag{46}$$

where the parameter u is expressed, with consideration of eqn (43), as follows:

$$u = kL = L\sqrt{2\pi r_0 \frac{\lambda_0}{\kappa}}. \tag{47}$$

Shearing stress. With the formulae (46) for the constants of integration, solution (13) results in the following expression for the shearing stress:

$$\tau_0(x) = \frac{P\lambda_0}{k\kappa}\frac{\cosh k(L-x)}{\sinh u}. \tag{48}$$

The stresses at the specimen's ends are

Table 1. Sensitivity factor and its derivative as functions of the radii ratio $\gamma_0 = r_1/r_0$

γ_0	1.5	1.4	1.3	1.2	1.1	1.05	1.01
η	1.570	1.724	1.952	2.342	3.239	4.527	10.025
$-\frac{d\eta}{d\gamma_0}$	1.412	2.123	2.932	4.571	9.538	19.520	99.504

$$\tau_0(0) = \frac{P\lambda_0}{k\kappa}\operatorname{cotanh} u, \quad \tau_0(L) = \frac{P\lambda_0}{k\kappa}\frac{1}{\sinh u}. \tag{49}$$

For long specimens with stiff interfaces, the parameter u is large, the stress $\tau_0(L)$ at the free end $x = L$ is very small, and the stress $\tau_0(0)$ at the origin, where the external force P is applied, is

$$\tau_0(0) = \frac{P\lambda_0}{k\kappa} = \frac{kP}{2\pi r_0} = k_L\frac{P}{2\pi r_0 L}. \tag{50}$$

Here $k_L = u = kL$ is the stress concentration factor.

The tensile force $T(x)$ can be determined by introducing eqn (38) into eqn (39):

$$T(x) = P\frac{\sinh k(L-x)}{\sinh u}. \tag{51}$$

When the u value is large, formulae (48) and (51) yield

$$\tau_0(x) = \frac{P\lambda_0}{k\kappa}e^{-kx}, \quad T(x) = Pe^{-kx}, \tag{52}$$

i.e. both the interfacial stress and the tensile force decrease exponentially with an increase in the distance x from the origin. For small u values, the formulae (48) and (51) result in equations which coincide with the first two equations in (31).

Stress sensitivity

Using the first formula in (21) and formula (49), and assuming $\nu_1 = 0.5$, we obtain the following formula for the maximum shearing stress:

$$\tau_{max} = \tfrac{1}{2}\eta\sigma_0\sqrt{\frac{2}{3}\frac{E_1}{E}}, \tag{53}$$

where $\sigma_0 = P/\pi r_0^2$ is the "nominal" tensile stress in the glass fiber, the factor

$$\eta = \frac{1}{\sqrt{\ln \gamma_0}} \tag{54}$$

considers the effect of the primary coating thickness, and the E value is equal to Young's modulus E_0 of the glass, in the case of a fiber embedded into epoxy adhesive, and to $E_2[(r_2^2 - r_1^2)/r_0^2]$, in the case of a specimen loaded at its end planes.

From eqn (54) we find, by differentiation,

$$\frac{d\eta}{d\gamma_0} = -\frac{1}{\gamma_0 \ln \gamma_0} = -\eta^2 e^{-1/\eta^2}. \tag{55}$$

The calculated values of the factor η and its derivative $d\eta/d\gamma_0$ are given in Table 1 and

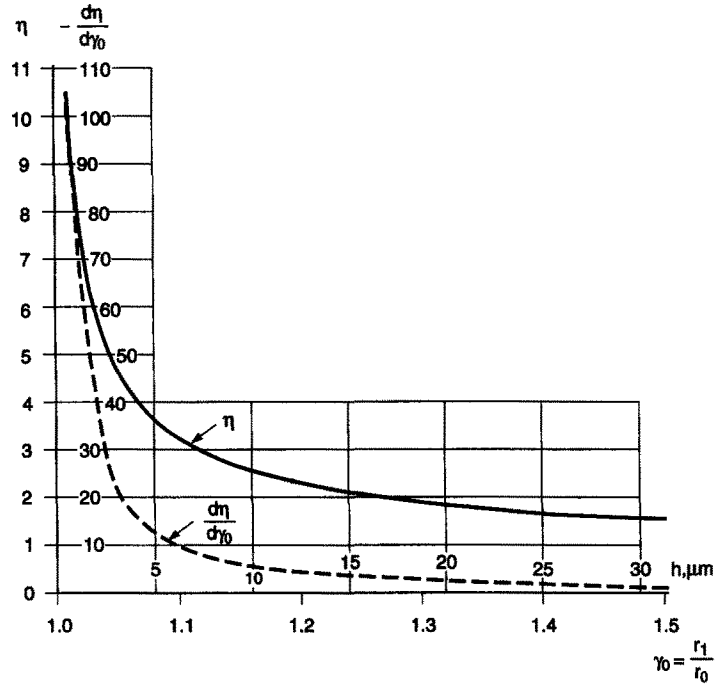

Fig. 4. Sensitivity factor and its derivative as functions of the radii ratio $\gamma_0 = r_1/r_0$ (the primary coating thickness is $h = r_1 - r_0$) for fiber radius $r_0 = 62.5$ μm.

plotted in Fig. 4 as a function of the radii ratio γ_0 and the primary coating thickness h (for the fiber radius of $r_0 = 62.5$ μm). As is evident from the calculated data, the maximum shearing stress increases with a decrease in the thickness of the primary coating, especially when this thickness is small (i.e. when the ratio γ_0 is close to unity). In addition, when the primary coating is thin, the maximum stress becomes highly sensitive to the change in the coating thickness. Indeed, in this case the factor η is large and formula (49) yields

$$\frac{d\eta}{d\gamma_0} = -\eta^2,$$

i.e. the absolute value of the derivative $d\eta/d\gamma_0 = r_0(d\eta/dh)$ increases as the factor η squared. This can, particularly, lead to high variability of the measured peak force in fibers with very thin coatings. A similar situation is thought to be possible in specimens with an elevated eccentricity in the position of the glass fiber with respect to the axis of the secondary coating. In such cases, pull-out tests may not be a good indicator of the adhesive strength of the primary coating, and therefore other means of measuring this strength should be considered.

Another way to approach the sensitivity problem is to assess the variability of the force P itself. From the first formula in (49) we obtain

$$P = 2\pi r_0 L \tau_{\max} \frac{\tanh u}{u}, \tag{56}$$

where the parameter u is expressed as

$$u = \eta L \sqrt{2\pi\lambda_0 G_1}$$

and the factor η, considering the effect of the primary coating thickness, is given by eqn (49). From eqn (51) we find

$$\frac{dP}{d\eta} = 2\pi r_0 L^2 \tau_{max} \sqrt{2\pi\lambda_0 G_1}\, \frac{u - \sinh u \cosh u}{u^2 \cosh^2 u}.$$

When the primary coating is thick, the radii ratio γ_0 is large, the parameters η and u are small, and the derivative $dP/d\eta$ is close to zero. This means that, in such a case, the change in the coating thickness does not lead to an appreciable change in the tensile force. However, when the primary coating is thin, the radii ratio γ_0 is close to unity and because of that the η and u values are large. Then we obtain

$$\frac{dP}{d\gamma_0} = \frac{dP}{d\eta}\eta^2 = -2\pi r_0^2 \sqrt{1+\nu_1}\, \tau_{max} \sqrt{\frac{E_0}{E_1}}. \tag{57}$$

This formula indicates that, since the moduli ratio E_0/E_1 is large, the derivative $dP/d\gamma_0$ is large as well, and increases with an increase in the adhesive strength of the primary coating (this strength is characterized by τ_{max} value). Hence, high variability of the pull-out force can be regarded as an indirect indication of a rather high interfacial strength.

Young's modulus evaluation

The maximum displacement of the glass fiber embedded into an adhesive can be evaluated, using the first formula in (49), as

$$w_0 = \kappa\tau_0(0) = \frac{P\lambda_0}{k} \operatorname{cotanh} u = P\lambda_0 L \frac{\operatorname{cotanh} u}{u}. \tag{58}$$

On the other hand, using eqns (3) and (47), we find that Young's modulus E_1 of the primary coating can be expressed through the parameter u by the formula

$$E_1 = \frac{1+\nu_1}{\pi\lambda_0 L^2} u^2 \ln \gamma_0. \tag{59}$$

The dimensionless spring constant

$$K = \frac{P\lambda_0 L}{w_0} = u \tanh u$$

is plotted in Fig. 5 as a function of the parameter u, which, as follows from eqn (59), can be expressed through the modulus E_1 as follows:

$$U = L\sqrt{\frac{E_1\lambda_0}{(1+\nu_1)\ln\gamma_0}}. \tag{60}$$

In the case of very short specimens and/or very compliant primary coatings, the u value is small and the K value becomes approximately equal to u^2. Then Young's modulus can be calculated by the simplified formula

$$E_1 = (1+\nu_1)\frac{P}{w_0}\frac{\ln\gamma_0}{L}. \tag{61}$$

This formula can be used for the u values not exceeding, say, 0.25. Note that, in this case, the glass fiber can be considered absolutely rigid and therefore its compliance λ_0 does not enter formula (61).

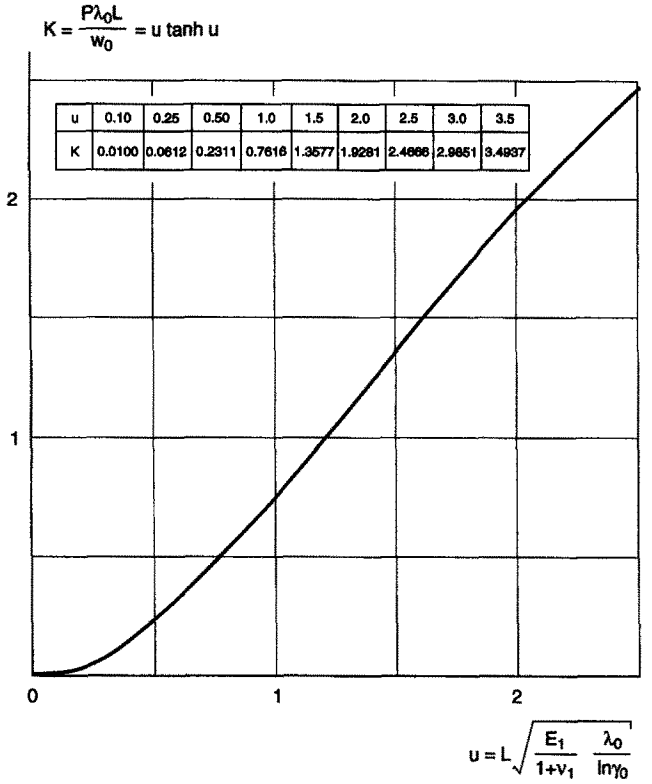

Fig. 5. Dimensionless longitudinal spring constant for a dual-coated fiber subjected to tension.

In the case of relatively long specimens and/or stiff primary coatings, the u value is large. In such a case the dimensionless spring constant K becomes approximately equal to u and Young's modulus of the primary coating can be evaluated as

$$E_1 = (1+\nu_1)\lambda_0\left(\frac{P}{w_0}\right)^2 \ln \gamma_0. \tag{62}$$

As is evident from this formula, calculated Young's modulus is independent of the specimen's length, but is affected by the axial compliance of the glass fiber. Formula (62) can be applied for u values larger than, say, 2.5.

For the u values in the region between 0.25 and 2.5, Young's modulus of the primary coating can be calculated on the basis of the plot in Fig. 5. In this case one should determine first the dimensionless spring constant K for the given length of the specimen L, the calculated axial compliance λ_0 of the glass fiber, the applied force P and the measured axial displacement w_0 of the glass fiber. Then, using the plot in Fig. 5, one can determine the corresponding u value and compute the modulus E_1 by formula (59).

Fiber strippability

Strippability requirements. In order to connect optical fibers to one another or to electronic equipment, it is usually necessary to remove the coating from short sections at the ends. Therefore, it is imperative that coated optical fibers have good strippability, i.e. lend themselves to easy mechanical removal of the coating. Clearly, the requirement for good strippability in coated optical fibers is in contradiction with the need for good adhesion of the primary coating to the glass. Since such an adhesion is thought to be crucial for reliable performance of the fibers, it cannot be compromised for the sake of good strippability. This provides an obvious challenge for manufacturing and design engineers; the stripping technology and tools must ensure a reliable stripping process no matter how strong the

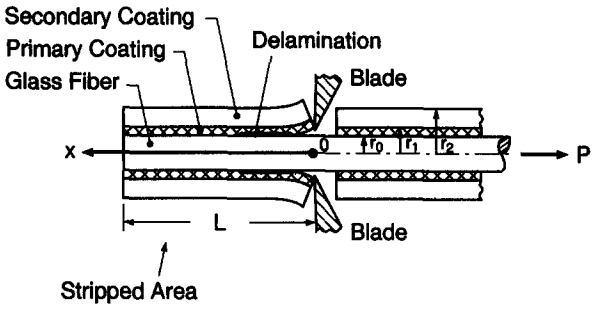

Fig. 6. Optical fiber specimen subjected to stripping.

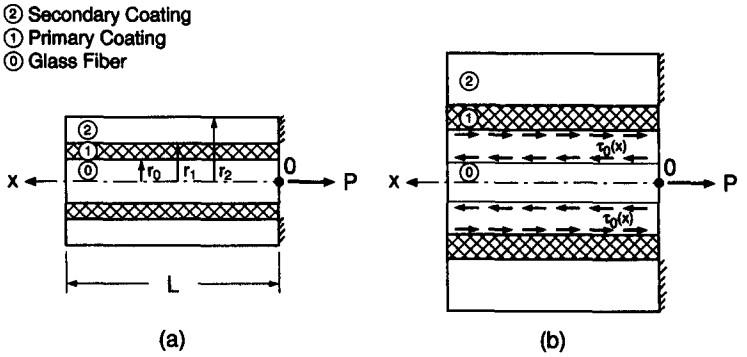

Fig. 7. Distributed shearing stress in an optical fiber subjected to stripping.

coating adhesion might be. A simple analytical stress model, which is set forth below, can be helpful in the assessment of the effect of Young's moduli and the thickness of the coating layers on the magnitude and distribution of the interfacial shearing stress responsible for the coating strippability. The effects of buckling (if any) of the secondary coating on the redistribution of the interfacial shearing stress, of the "residual" thermally induced stresses, and of the fracture toughness of the primary coating material (i.e. its ability to withstand the initiation and propagation of the delamination) are not considered in this model.

Shearing stress. The shearing stress $\tau_0(x)$ on the glass surface of a dual-coated optical fiber subjected to stripping (Figs 6 and 7) can be determined on the basis of condition (2), where the interfacial displacements $w_0(x)$ and $w_2(x)$ of the glass fiber and the secondary coating can be expressed, on the basis of Hooke's law, as follows:

$$w_0(x) = \lambda_0 \int_0^x T_0(\xi)\,d\xi, \quad w_2(\alpha) = \lambda_2 \int_x^L T_0(\xi)\,d\xi. \tag{63}$$

Here L is the length subjected to stripping, $T_0(x)$ is the axial force in the glass fiber, given by formula (5), and λ_0 and λ_2 are the axial compliances of the glass fiber and the secondary coating. These can be evaluated by formulae (7). Introducing eqn (63) into the compatibility condition (2), we obtain

$$\lambda_2 \int_x^L T_0(\xi)\,d\xi - \lambda_0 \int_0^x T_0(\xi)\,d\xi = \kappa\tau_0(x). \tag{64}$$

By differentiating this relationship with respect to x, we have

$$-\lambda T_0(x) = \kappa \tau_0'(x), \tag{65}$$

where $\lambda = \lambda_0 + \lambda_2$ and κ is the interfacial compliance, expressed by eqn (3). The next differentiation of eqn (65), with consideration of formula (5), results in eqn (11), and the solution to this equation is given by expression (13). The constants C_1 and C_2 of integration can be found from the boundary conditions (14) for the force $T_0(x)$. These conditions, with considerations of the relationship (65), yield

$$\tau_0'(0) = -\frac{\lambda P}{\kappa}, \quad \tau_0'(L) = 0. \tag{66}$$

Note that they are different from conditions (15), because expressions (63) for the displacements are different. Substituting eqn (13) into conditions (66), we find

$$C_1 = \frac{\lambda P}{k\kappa}, \quad C_2 = \frac{\lambda P}{k\kappa} \operatorname{cotanh} u, \tag{67}$$

where the parameter u is expressed by eqn (17). With formulae (67), solution (13) can be written as follows:

$$\begin{aligned} \tau_0(x) &= \frac{\lambda P}{k\kappa}(\operatorname{cotanh} u \cosh kx - \sinh kx) \\ &= \frac{kP}{2\pi r_0}(\operatorname{cotanh} u \cosh kx - \sinh kx). \end{aligned} \tag{68}$$

The maximum and minimum shearing stresses occur at the ends ($x = 0$ and $x = L$) of the stripping area:

$$\tau_{\max} = \tau_0(0) = \frac{kP}{2\pi r_0} \operatorname{cotanh} u \tag{69}$$

$$\tau_{\min} = \tau_0(L) = \frac{kP}{2\pi r_0} \frac{1}{\sinh u}. \tag{70}$$

As is evident from formula (69), the maximum shearing stress at the origin, i.e. at the cross-section of the application of the blades, changes from

$$\tau_\infty = \frac{kP}{2\pi r_0}, \tag{71}$$

for long stripping areas ($u > 2.5$), to

$$\tau_0 = \frac{P}{2\pi r_0 L} \tag{72}$$

for short areas ($u < 0.3$). The minimum shearing stress, as is evident from formula (70), changes to zero, in the case of an infinitely long stripping area ($u \to \infty$), to the value defined by formula (72), in the case of a short stripping area. Certainly, in the latter case, the shearing stress can be considered more or less uniformly distributed over the length of the stripping area.

It should be pointed out that the maximum stress $\tau_{\max}$ expressed by formula (69) is independent of the length of the stripping area and is larger than the average stress τ_0, given by formula (72), only if the stripping area is sufficiently long. In the case of a short stripping area, the interfacial shearing stress, as has been indicated above, is more or less

uniform and, as is evident from formula (72), can be rather significant if the length L is small. It is no wonder that, in the case of short stripping areas, stripping does not typically encounter any difficulties (Simoff, 1992). Since good strippability can be expected for short stripping areas, characterized by high and more or less uniformly distributed shearing stresses and satisfactory elastic stability of the secondary coating, we suggest that in a situation when a long area of the coated fiber must be stripped, a multiblade stripping tool be considered. In such a tool, the distance between the blades should be made equal to the predicted or measured length of the stripping area for which good strippability is expected or achieved.

It is noteworthy that formulae (71) and (72) indicate that the parameter

$$u = \frac{\tau_{max}}{\tau_0} = kL \tag{73}$$

defined by formula (17) is, in effect, a stress concentration factor.

Axial force. The axial force $T_0(x)$ in the secondary coating at an arbitrary cross-section x can be found, on the basis of formulae (5) and (68), as follows:

$$T_0(x) = P(\cosh kx - \operatorname{cotanh} u \sinh kx). \tag{74}$$

For sufficiently long stripping areas ($u > 2.5$), this formula yields

$$T_0(x) = Pe^{-kx}, \tag{75}$$

i.e. the tensile force in the glass fiber and the compressive force in the secondary coating decrease exponentially with an increase in the distance x from the origin. The compressive force decreases faster in the case of large k values, i.e. for more compliant secondary coatings and stiffer (thinner, with higher Young's moduli) primary coatings.

For very short stripping areas ($u < 0.3$), formula (74) yields

$$T_0(x) = P\left(1 - \frac{x}{L}\right), \tag{76}$$

i.e. the axial force in the glass fiber and in the secondary coating decreases linearly with an increase in the distance x from the origin.

The shearing stress $\tau_0(x)$ can be determined, on the basis of formula (5), as follows:

$$\tau_0(x) = -\frac{1}{2\pi r_0}\frac{dT_0(x)}{dx}.$$

In the case of long stripping areas, when the force $T_0(x)$ is expressed by formula (75), we obtain

$$\tau_0(x) = \frac{kP}{2\pi r_0}e^{-kx},$$

i.e. the shearing stress concentrates at the origin and rapidly fades away with an increase in the distance x from the origin. In the case of a short stripping area, when the force $T_0(x)$ is expressed by formula (76), the shearing stress is

$$\tau_0(x) = \frac{P}{2\pi r_0 L},$$

i.e. distributed uniformly along the stripping area.

Discussion. High interfacial shearing stress at the cross-section where the blades are located and a more or less uniform distribution of the interfacial shearing stress along the stripping area are thought to have a favorable effect on fiber strippability. High shearing stress at the loaded end eases the desirable "local" adhesive failure (delamination) of the primary coating material. Such a failure is needed to trigger (initiate) delamination. Obviously, for the given stress at the origin, a more uniform distribution of the interfacial shearing stress along the stripping area (resulting in higher stresses at the free end) eases the propagation of this delamination, i.e. makes the delamination "global". It is clear also that if the stripping area is long enough, the requirements that the maximum shearing stress at the origin be high and, at the same time, the shearing stress is more or less uniformly distributed over the length of the stripping area, are in contradiction. High stress concentration near the loaded end (high maximum stress at the blade and a short area experiencing elevated stresses) can have a favorable effect on fiber strippability only in the case of very short stripping areas, in which a more or less uniform stress distribution is achieved anyway. However, for stripping lengths of practical interest (exceeding, say, 10 mm) the uniformity of the stress distribution along the stripping area is usually more important than the high stress level at the loaded end (unless the coating adhesion is significant and the propensity of the primary coating material to delamination is not very high, so that a high maximum stress at the blades location is needed to initiate delamination), and therefore high stress concentration should be viewed as far as the coating strippability is concerned, as an adverse factor.

Buckling of the secondary coating during stripping can have either a positive or a negative effect on the strippability, depending on the adhesive strength of the primary coating, its ability to withstand the initiation and propagation of delamination, sign and level of any thermally induced stresses, etc. It is our feeling that the overall effect of buckling, from the strippability viewpoint, is such that it should be regarded as an adverse, rather than a favorable factor. Indeed, buckling of the secondary coating (which is more likely for long stripping areas) results in a situation where a large portion of the external work due to the movement of the blades (or pulling the glass fiber) leads to the accumulation of strain energy in the post-buckled secondary coating. Only a small portion of this work then contributes to the desirable increase in the strain energy of the primary coating and its potential failure. Buckling of the secondary coating leads to a strongly pronounced nonuniform (quasi-periodic) longitudinal distribution of the interfacial shearing stress. This may contribute to the observed residue patterns of the primary coating material on the surface of the stripped fiber (Simoff, 1992). Such residues are more likely in the areas remote from the origin, where the interfacial shearing stresses are relatively low. Although satisfactory delamination is often achieved even in the presence of buckling (especially if the primary coating experiences radial thermally induced tensile stresses and has poor adhesion to the glass), it is still preferable that the stripping area be so short that the elastic stability of the secondary coating is not compromised.

For long stripping areas, as is evident from formula (71), the maximum shearing stress at the origin increases for a given external force P, with an increase in the magnitude of the parameter k. This parameter, as one can see from formula (12), increases with an increase in the total axial compliance λ of the glass coating composite and a decrease in the interfacial compliance κ. Since, as it follows from formulae (7) and (9), the total axial compliance λ is due primarily to the secondary coating (the axial compliance λ_0 of the glass is substantially smaller than the compliance λ_2 of the secondary coating), a decrease in Young's modulus and the cross-sectional area of this coating (resulting in its higher axial compliance) leads to a higher stress at the origin. Physically, this can be explained by the fact that compliant secondary coatings transmit the external load P to the surface of the glass fiber within a

shorter region than stiff (rigid) coatings, thereby resulting in higher shearing stresses at the glass fiber surface.

The interfacial shearing compliance κ, which is due primarily to the primary coating, decreases, as follows from eqn (3), with a decrease in the primary coating thickness and an increase in the shear modulus (Young's modulus) of the material. Since thinner primary coatings with higher Young's moduli result in higher shearing stresses, a decrease in the primary coating thickness and an increase in Young's modulus of the material have a favorable effect on fiber strippability in the case of a very short stripping area, but adversely affect the strippability if the stripping section is long.

It is noteworthy that, although the "residual" thermally induced stresses [see, for instance, Suhir (1988b)] in the primary coating material could be substantially lower than the stresses due to mechanical stripping, thermal stresses can make a difference, as far as the fiber strippability is concerned. Clearly, tensile thermally induced stresses, which are undesirable from the standpoint of the adhesive strength of the primary coating, can improve the coating strippability. It is important also, to what extent the adhesion of the primary coating to the glass fiber is due to the thermal and the chemical forces (bonding). The strippability seems to be better in a situation when the "adhesion" is due primarily to thermal (mechanical) forces. Obviously, good stripping is easier to achieve if there is no chemical bonding of the primary coating to the glass fiber.

NUMERICAL DATA

1. Let a 1 cm long optical fiber specimen ($r_0 = 62.5$ μm, $E_0 = 10.4 \times 10^6$ psi $= 7.167 \times 10^{10}$ Pa) be subjected to a $P = 2$ kg $= 19.6$ N tensile force. With $r_2 = 127.5$ μm, $E_2 = 150{,}000$ psi $= 1.034 \times 10^9$ Pa and a 29.5 μm thick primary coating ($E_1 = 100$ psi $= 6.892 \times 10^5$ Pa, $\nu_1 = 0.5$), we obtain: $\lambda_0 = 0.001137$ 1/N, $\lambda_2 = 0.0395$ 1/N, $\lambda = 0.0406$ 1/N, $\kappa = 1.052 \times 10^{-10}$ m^3/N.

In the case of a specimen loaded at its end planes, the calculated eigenvalue k is $k = 389.5$ 1/m and the parameter u is $u = kL = 3.895$. Then the calculated maximum stress, predicted on the basis of the second formula in (19), is $\tau_{max} = 1.890 \times 10^7$ Pa $= 1.932$ kg/mm^2, and the maximum axial displacement of the glass fiber is $w_0 = \kappa\tau_{max} = 1.99$ mm.

In the case when the specimen is embedded into an epoxy adhesive, the eigenvalue k is $k = 65.1$ 1/m and the stress concentration factor is $u = kL = 1.137$, i.e. significantly smaller than for a specimen loaded at its end planes. The maximum shearing stress predicted using the first formula in (49) is $\tau_{max} = 0.5684 \times 10^7$ Pa $= 0.580$ kg/mm^2 and the maximum displacement of the glass fiber is $w_0 = 0.60$ mm. Note that the length of a specimen which would result in practically uniform distribution of the shearing stress, is characterized by the u value not exceeding 0.25 and is about $L = 0.25/k = 3.8$ mm.

The distributed shearing stresses calculated on the basis of formulae (18) and (48) are shown in Figs 2(a) and 3(a). The predicted stresses are in good agreement with the results of finite element computations. In these computations the ANSYS package was used and an axisymmetric preprocessing model was applied.

2. Examine now a hypothetical case of a very thin coating. If the thickness of the primary coating is reduced from 29.5 μm to, say, 10 μm, then the calculated interfacial compliance reduces to $\kappa = 0.404 \times 10^{-10}$ m^3/N. In the case of a specimen loaded at its end planes, we obtain $k = 628.2$ 1/m, $u = kL = 6.282$, $\tau_{max} = 3.051 \times 10^7$ Pa $= 3.113$ kg/mm^2 and $w_0 = 1.23$ mm. For a specimen embedded into epoxy, we have $k = 105.1$ 1/m, $u = 1.051$, $\tau_{max} = 0.671 \times 10^7$ Pa $= 0.684$ kg/mm^2, $w_0 = 0.271$ mm. Thus, the decrease in the primary coating thickness resulted in the increase in the maximum shearing stress by a factor of 1.61 in the case of a specimen loaded at its end planes, and by a factor of 1.18 in the case of a specimen embedded into an epoxy adhesive. The length of a specimen which would result in a practically uniform distribution of the shearing stress is about $L = 0.25/k = 2.4$ mm, i.e. substantially smaller than for a specimen with a normal (thick) primary coating.

The distributed stresses calculated on the basis of formulae (18) and (48) are shown in Figs 2(b) and 3(b).

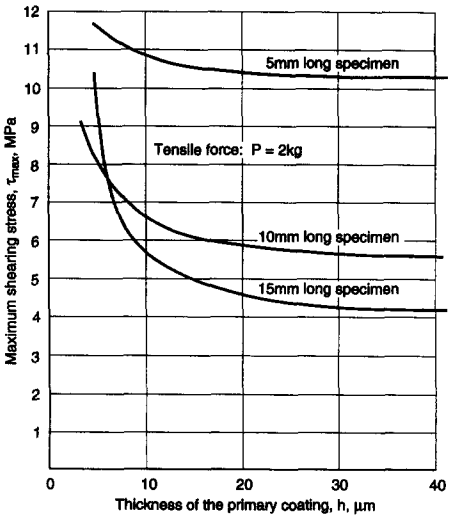

Fig. 8. Predicted maximum shearing stress as a function of the primary coating thickness h for different specimen lengths and a 2 kg tensile force.

3. The predicted maximum stresses for a 2 kg tensile force are shown as a function of the primary coating thickness for different specimen lengths in Fig. 8 for the case of a specimen embedded into an epoxy. As is evident from this figure, employment of 1 cm long specimens with 29.5 μm thick primary coatings is acceptable, however, shorter specimens result in a more uniform shearing stress and therefore are more preferable. Application of short specimens can become necessary in a hypothetical case of a fiber with very thin primary coatings (thinner than, say, 10 μm).

4. Let us show how the obtained results can be applied to evaluate Young's modulus of the primary coating from the measured axial displacement w_0 of the glass fiber. Let the measured displacement in a 10 mm long specimen with a 29.5 μm thick primary coating be $w_0 = 3$ μm for a $P = 10$ g $= 0.098$ N tensile force. Then we obtain $K = P\lambda_0 L/w = 0.3714$. In accordance with the data for Fig. 5, the corresponding u value is about 0.65. With the radii ratio $\gamma_0 = 1.472$ (which corresponds to the thickness of the primary coating of 29.5 μm), assuming $\nu_1 = 0.5$ and using formula (59), we obtain $E_1 = 0.0700$ kg/mm^2 = 686 kPa = 99.6 psi. The finite element computations with the input data $P = 10$ g, $E_1 = 100$ psi, $\nu_1 = 0.499$ and $\gamma_0 = 1.472$ resulted in an axial displacement of 3.0 μm, which coincides with the prediction based on an analytical stress model.

5. Let a 30 mm long optical fiber specimen ($r_0 = 62.5$, $E_0 = 10.4 \times 10^6$ psi $= 7.167 \times 10^{10}$ Pa) be subjected to a $P = 2$ kgf $= 19.6$ N stripping force. With $r_2 = 127.5$ μm, $E_2 = 150{,}000$ psi $= 1.034 \times 10^9$ Pa and 29.5 μm thick primary coating ($E_1 = 100$ psi $= 6.892 \times 10^5$ Pa, $\nu_1 = 0.5$), one can obtain $\lambda_0 = 0.001137$ 1/N, $\lambda_2 = 0.0395$ 1/N, $\lambda = 0.0406$ 1/N, $\kappa = 1.052 \times 10^{-10}$ m^3/N. The eigenvalue k, calculated on the basis of formula (12), is $k = 389.5$ 1/m, and the parameter u is $u = kL = 11.685$. This value is very large, so that the shearing stress is distributed quite nonuniformly along the stripping area. Its maximum value (at the blade cross-section), predicted by formulae (69) and (70), is $\tau_{max} = 1.9837$ kgf/mm^2 = 2821 psi, while the value of the shearing stress at the free end is practically zero. As follows from formula (75), the shearing stress (force) is only 1% of its value at the origin at the distance $L = -(\ln 0.01/k) = 11.8$ mm. This result indicates that satisfactory strippability can be expected if the length of the stripping area is appreciably smaller than 11.8 mm.

Clearly, the best strippability can be achieved if the entire stripping area is subjected to elevated and uniformly distributed shearing stresses. Based on formula (69), it is desirable that the length L of the stripping area be sufficiently small to achieve uniform interfacial shearing stress. This will happen if the relationship $\operatorname{cotanh} u \approx 1/u$ (or $\tanh u \approx u$) is fulfilled. This yields $u < 0.3$ so that $L = 0.3/k = 0.770$ mm.

A less conservative (and more practical) assessment of the length required for satisfactory strippability can be done assuming that, say, 10% of the shearing stress at the origin is transmitted to the free end. This results in a length of $L = 3.0/K = 7.7$ mm. The maximum shearing stress in this case is $\tau_{max} = 1.9936$ kgf/mm^2, i.e. somewhat higher than for a very long stripping area. This is, however, not as important as the fact that the entire length of this area is subjected to elevated shearing stresses. Clearly, if a multiblade stripping tool, with the distance between the blades of about 8 mm, is used, then the strippability of a fiber with a long stripping area should be expected to be as good as the strippability of a fiber with a stripping area of 7.7 mm.

CONCLUSIONS

The following major conclusions can be drawn from the performed analysis.

- In a cylindrical double lap shear joint (dual-coated optical fiber specimen), the interfacial shearing stress is distributed nonuniformly over its length and its maximum value increases with a decrease in the thickness of the primary coating.
- An increase in Young's modulus and the cross-sectional area of the secondary coating result in a more uniform distribution of the shearing stress along the specimen and in lower maximum stresses. Therefore, the expected stresses in a specimen embedded into an epoxy adhesive are lower and are more uniformly distributed over the specimen's length than in a specimen loaded at its end planes. Our calculations showed that employment of 1 cm long specimens with approximately 30 μm thick low modulus primary coating is acceptable, however, shorter specimens, resulting in a more uniform distribution of the shearing stress, are preferable.
- The results of the performed analysis for the pull-out testing are in good agreement with finite element computations and with the existing experimental data. These results can be used when comparing the adhesive strength of the primary coating material in specimens with different coating designs, or in specimens of different lengths. They can also be helpful when choosing the appropriate specimen length for the given coating materials and cross-sectional geometry.
- The shearing stress at the point of the blade location, arising during stripping of optical fiber coating, decreases and the length subjected to elevated shearing stresses increases with a decrease in Young's modulus of the primary coating material and an increase in the coating's thickness and Young's modulus of the secondary coating. For stripping lengths of practical interest (exceeding, say, 10 mm), the uniformity of the stress distribution along the stripping area is more important than the high stress level at the loaded end, so that low stress concentration near the blade should be viewed as a positive factor, as far as the strippability of long areas is concerned.
- A high and uniformly distributed interfacial shearing stress, desirable from the viewpoint of good strippability of dual-coated fibers, can be obtained in the case of short stripping areas, not exceeding a few millimeters. For a given external force, this stress increases with an increase in Young's modulus of the primary coating and a decrease in Young's modulus of the secondary coating. A decrease in the thickness of either of the coating layers results in higher interfacial stresses. A high stress at the loaded end, is thought to have an adverse effect on long stripping portions. However, high stress should be beneficial for very short stripping areas because the short length results in a more or less uniform distribution of stresses. The requirements for high and uniformly distributed stresses would not be mutually exclusive if the stripping area were sufficiently short. Therefore, we suggest that a multiblade stripping tool be used in those cases where a longer stripping area is needed. If such a tool is considered, the distance between the blades should be made equal to the predicted or measured length of the stripping area for which good strippability is expected or achieved. The numerical example carried out for a typical dual-coated optical fiber indicates that good strippability can be expected if the length of the stripping area does not exceed 8–10 mm.

- The results of the performed analysis for the coating strippability can be used to evaluate the effect of material and geometry characteristics on the magnitude and the distribution of the interfacial shearing stresses responsible for the strippability of a dual-coated optical fiber. The obtained formulae can also be used to establish the appropriate distance between the blades in a multiblade stripping tool.

Acknowledgements—The author is thankful to D. A. Simoff and L. L. Blyler, Jr for useful comments and to A. Koert for carrying out finite element computations.

REFERENCES

Aleck, B. J. (1949). Thermal stresses in a rectangular plate clamped along an edge. *ASME J. Appl. Mech.* **16,** 118–122.

Chang, F.-V. (1983). Thermal contact stresses of bi-metal strip thermostat. *Appl. Math. Mech.* **4**(3), 363–376.

Chen, W. T. and Nelson, C. W. (1979). Thermal stress in bonded joints. *IBM J. Res. Dev.* **23**(2), 179–188.

Du Chen, S. C. (1983). An analysis of adhesive-bonded single-lap joints. *ASME J. Appl. Mech.* **50,** 110–115.

Goland, M. and Reissner, E. (1944). The stresses in cemented joints. *ASME J. Appl. Mech.* **11,** 17–27.

Grimado, P. B. (1978). Interlaminar thermoelastic stresses in layered beams. *J. Thermal Stresses* **1,** 75–86.

Mishkevich, V. and Suhir, E. (1993). Simplified engineering approach for the evaluation of thermally induced stresses in bi-material microelectronic structures. In *Structural Analysis in Microelectronic and Fiber Optics* (Edited by E. Suhir), Vol. 7, pp. 127–133. Van-Nostrand Reinhold, New York.

Overton, B. J. and Taylor, C. R. (1989). Time–temperature dependence of dual-coated lightguide pull-out measurements. *Polym. Engng Sci.* **29** (17), 1169–1171.

Simoff, D. (1992). AT & T Bell Laboratories, Murray Hill, NJ. Personal communication.

Suhir, E. (1986). Stresses in bi-metal thermostats. *ASME J. Appl. Mech.* **53**(3), 657–660.

Suhir, E. (1988a). Thermal stress failures in microelectronic components—review and extension. In *Advances in Thermal Modeling of Electronic Components and Systems* (Edited by A. Bar-Cohen and A. D. Kraus), Vol. 1, pp. 337–412. Hemisphere, New York.

Suhir, E. (1988b). Stresses in dual-coated optical fibers. *ASME J. Appl. Mech.* **55**(10), 822–830.

Suhir, E. (1989). Interfacial stresses in bi-metal thermostats. *ASME J. Appl. Mech.* **56**(3), 595–600.

Suhir, E. (1991). Approximate evaluation of the elastic interfacial stresses in thin films, with application to high-T_c superconducting ceramics. *Int. J. Solids Structures* **27**(8), 1025–1034.

Suhir, E. and Sullivan, T. M. (1990). Analysis of the interfacial thermal stresses and adhesive strength of bi-annular cylinders. *Int. J. Solids Structures* **26**(5/6), 581–599.

Taylor, C. R. (1985). *In situ* mechanical measurements of optical fiber coatings. *Conf. Optical Fiber Commun.* Technical Digest MG-5, San-Diego, CA.

Volkersen, O. (1938). Die Nietkraftverteilung in zubeanspruchten Nietverbindungen mit konstanten Laschonquerschnitten. *Luftfahrforschung* **15,** 41–45 (in German).